PROCEEDINGS OF SCIENCE

The 3-state Potts model as a heavy quark finite density laboratory

Seyong Kim[*†]
Department of Physics, Sejong University, Seoul 143-747, Korea
Department of Physics, U. of Wales Swansea, Swansea SA2 8PP, U.K.
E-mail: skim@sejong.ac.kr

Ph. de Forcrand
Institut für Theoretische Physik, ETH-Zürich, CH-8093 Zürich, Switzerland
CERN Theory Division, CH-1211 Geneva 23, Switzerland
E-mail: forcrand@phys.ethz.ch

S. Kratochvila
Institut für Theoretische Physik, ETH-Zürich, CH-8093 Zürich, Switzerland
E-mail: skratoch@phys.ethz.ch

T. Takaishi
Hiroshima U. of Economics
Hiroshima 731-0124, Japan
E-mail: takaishi@hiroshima-u.ac.jp

The 3-D Z(3) Potts model is a model for finite temperature QCD with heavy quarks. The chemical potential in QCD becomes an external magnetic field in the Potts model. Following Alford et al.[3], we revisit this mapping, and determine the phase diagram for an arbitrary chemical potential, real or imaginary. Analytic continuation of the phase transition line between real and imaginary chemical potential can be tested with precision. Our results show that the chemical potential weakens the heavy-quark deconfinement transition in QCD.

XXIIIrd International Symposium on Lattice Field Theory
25-30 July 2005
Trinity College, Dublin, Ireland

[*]Speaker.

[†]S.K. is supported by Grant No. R01-2002-000-00291-0 from the Basic Research Program of Korea Science and Engineering Foundation

PoS(LAT2005)166

1. Introduction

The 3-dimensional 3-state Potts model and the finite temperature QCD with infinitely heavy quarks share the same $Z(3)$ global symmetry, and in both theories the order parameter shows a first order phase transition. When an external magnetic field is turned on in the Potts model, this $Z(3)$ symmetry is explicitly broken and the first order phase transition is weakened, becoming second order for a certain strength of the magnetic field and crossover beyond. In the case of finite temperature QCD, the quark mass plays the role of the external magnetic field in the 3-D 3-state Potts model. The first order phase transition of the quenched theory (infinitely heavy quark limit) weakens, and turns into a second order transition for a critical, heavy but not infinite, dynamical quark mass [1, 2]. A universality argument then implies that the critical properties of the two theories, Potts and QCD, will be the same at this second-order point. Since the 3-D 3-state Potts model is simpler than QCD and can be simulated on a large lattice, its numerical investigation will give us more detailed quantitative information on the critical properties of finite temperature QCD with heavy quarks.

The effect of a quark chemical potential on hot QCD with static quark sources can be formulated in the following grand canonical ensemble [3]:

$$\begin{aligned} Z(\mu) &= \sum_{n,\overline{n}} Z_{n,\overline{n}}\ e^{\beta\mu(n-\overline{n})} \\ &= \sum_{n,\overline{n}} \int [\mathscr{D}U]\ \frac{1}{n!}(\Phi[U])^n \frac{1}{\overline{n}!}\ (\Phi[U]^*)^{\overline{n}}\ e^{-S_g[U]-\beta n(M-\mu)-\beta\overline{n}(M+\mu)} \\ &= \int [\mathscr{D}U] \exp(-S_g[U] + e^{-\beta(M-\mu)}\Phi[U] + e^{-\beta(M+\mu)}\Phi[U]^*), \end{aligned} \tag{1.1}$$

where $Z_{n,\overline{n}}$ is the canonical partition function with n quarks and $\overline{n}$ anti-quarks, U is the SU(3) gauge field, S_g is the gauge action, Φ is the Polyakov line, Φ^* the anti-Polyakov line, M is the heavy quark mass and μ is the quark chemical potential. When there is no chemical potential ($\mu = 0$), the action in (1.1) is real. If $\mu \neq 0$, the action becomes complex and Monte Carlo simulation is difficult because of the "sign problem": the usual probabilistic interpretation of Eq. (1.1) is not possible.

Symmetry consideration tells us that the important dynamics of the gauge field are those of the Polyakov line and the anti-Polyakov line. Thus, the corresponding lattice Hamiltonian for the 3-D 3-state Potts model is given by:

$$H = -k\sum_{i,\vec{x}} \delta_{\Phi(\vec{x}),\Phi(\vec{x}+i)} - \sum_{\vec{x}} [h\Phi(\vec{x}) + h'\Phi^*(\vec{x})] \tag{1.2}$$

where $h = e^{-\beta(M-\mu)} = h_M e^{\beta\mu} = h_M e^{\overline{\mu}}$ and $h' = e^{-\beta(M+\mu)} = h_M e^{-\beta\mu} = h_M e^{-\overline{\mu}}$ with $h_M = e^{-M/T}$, $\overline{\mu} = \mu/T$, and $\Phi(\vec{x})$ is a $Z(3)$ spin. If $h \neq h'^*$, this Hamiltonian also is complex. However, the partition function remains real [3]. The partition function includes summation over all the possible $Z(3)$ spin configurations. Introducing "bonds" with a certain probability among parallel $Z(3)$ spins and defining a "cluster" made of the sites connected by the bonds, we can divide the summation into the sum over clusters and that within a cluster. Then, after analytically summing over $Z(3)$ spin orientations within each cluster, the partition function in terms of cluster configurations is given by

$$Z = \int [\mathscr{D}b](e^k - 1)^{N_b} \prod_C \left[e^{2h_M|C|\cosh\overline{\mu}} + 2e^{-h_M|C|\cosh\overline{\mu}} \cos(\sqrt{3}h_M|C|\sinh\overline{\mu}) \right], \tag{1.3}$$

where $\mathscr{D}b$ is the sum over all the possible bond configurations, N_b is the number of bonds in a given cluster configuration, and $|C|$ is the number of sites in a given cluster. Z is real and is free from the "sign problem" since the second term which can be negative due to the presence of $\cos(\sqrt{3}h_M|C|\sinh\overline{\mu})$ is always smaller than the first term. However, the "solution" of the complex action problem in the 3-D 3-state Potts model is different from the $SU(2)$ gauge theory case [6] and from the four-fermi theory case [7], where the action itself can be shown to be real even with a real chemical potential. In the Potts model, the action is complex, and a change of variables (from spins to bonds) is necessary to recover a real effective action and show that the partition function of the model remains real.

The $(h = h')$ case (that is, zero chemical potential) has been studied in [4]. The $(h' = 0)$ case (that is, $M, \mu \to \infty$ while M/μ is fixed) has been investigated in [3]. Since we are also interested in testing the analytic continuation of imaginary chemical potential results to real chemical potential, instead of taking $h' = 0$ limit, we study here the full parameter space of arbitrary (h, h').

For the case of an imaginary chemical potential ($\mu \to \mu_I$, i.e., $h' = h_M e^{-i\overline{\mu}_I} = h^*$), the partition function, Z_I, becomes

$$Z_I = \int \mathscr{D}b(e^k - 1)^{N_b} \prod_C \left[e^{2h_M|C|\cos\overline{\mu}_I} + 2e^{-h_M|C|\cos\overline{\mu}_I}\cosh(\sqrt{3}h_M|C|\sin\overline{\mu}_I) \right]. \tag{1.4}$$

Since $\cosh(i\overline{\mu}) = \cos(\overline{\mu}), \sinh(i\overline{\mu}) = i\sin(\overline{\mu})$ and $\cos(i\theta) = \cosh(\theta)$, the relation $Z(\mu \to i\mu_I) = Z_I(\mu_I)$ is quite obvious and the analytic continuation between Z and Z_I is transparent. The Roberge-Weiss symmetry [5], $Z_I(\frac{\mu_I}{T}) = Z_I(\frac{\mu_I}{T} + \frac{2\pi}{3}n)$, can also be seen clearly in (1.4).

2. Real Chemical Potential

Using the Swendsen-Wang cluster algorithm [8] on (1.3), we simulate the 3-D 3-state Potts model. The actual simulation is performed along the $h = h'$ line in the (h, h') parameter space and the data are re-weighted for arbitrary (h, h'). Although the reweighting factor is not always positive, this strategy is more efficient than sampling Eq. (1.3), because the ensuing sign problem is very mild. Simulations are performed on lattice volumes $56^3, 64^3$, and 72^3. Typically ~ 2 million data sample is collected. The critical point is located by requiring the third order Binder cumulant of the $Z(3)$ spin magnetization to vanish and by evaluating the fourth order Binder cumulant (B_4) of the magnetization at that point. Since the universality class of the 3-D 3-state Potts model is that of the 3-D Ising model, B_4 for the Potts model at the critical point should be equal to that of the Ising model ($= 1.604(1)$). Figure (1) shows the fourth order Binder cumulant as a function of h (here, $h' = h$). From this Figure, we find that the critical end point is at $(k_c, h_c) = (0.54940(4)0.000255(5))$ in comparison with the value given in [4], $(0.54938(2), 0.000258(3))$. Similarly, for the $h' = 0$ case, we obtain that $(k_c, h_c) = (0.54947(1), 0.000465(5))$ ([3] reported $(k_c, h_c) = (0.549463(13), 0.000470(2))$.

Similarly, the critical end point can be located for arbitrary h and h'. Figure (3) shows the (h, h') parameters for the second order phase transition. Here, instead of directly plotting (h, h'), we use variables M/T and μ/T, which can be related to QCD. The line in the figure is from the asymptotic value, $(h = h_c, h' = 0)$. Since $h = e^{-M/T+\mu/T}$, the relation $h_c = e^{-M/T+\mu/T}$ for given h_c defines a line in the parameter space $(\frac{M}{T}, \frac{\mu}{T})$. In Figure (3), the simulation data lies above this asymptotic

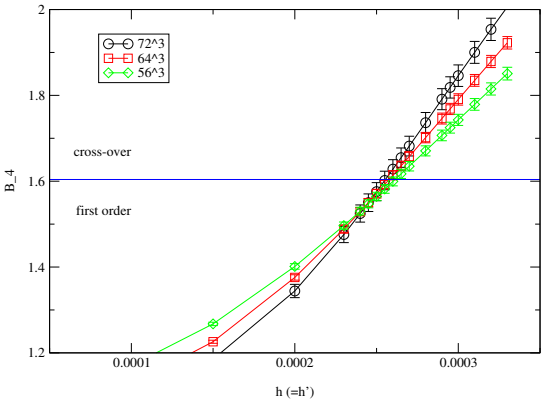

Figure 1: B_4 for magnetization vs h ($h = h'$)

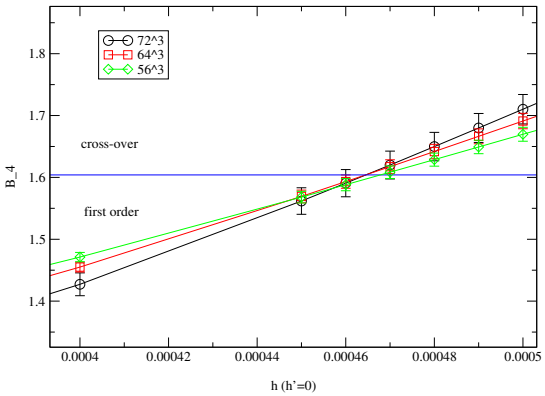

Figure 2: B_4 for magnetization vs h ($h' = 0$)

line. This means that the anti-Polyakov line in finite temperature QCD plays an important role in critical parameter space and should not be neglected in considering the critical properties of the theory. To further compare our results with the limit studied in [3], we show T/M vs. μ/M in Figure (4). As μ/M increases, our simulation data approach the asymptotic line as expected. This figure clearly shows that the range of T/M values for which the transition is first-order shrinks as the chemical potential is turned on. In fact, the transition disappears altogether for $\frac{\mu}{M} > 1$. So the effect of the chemical potential is to *weaken* the phase transition.

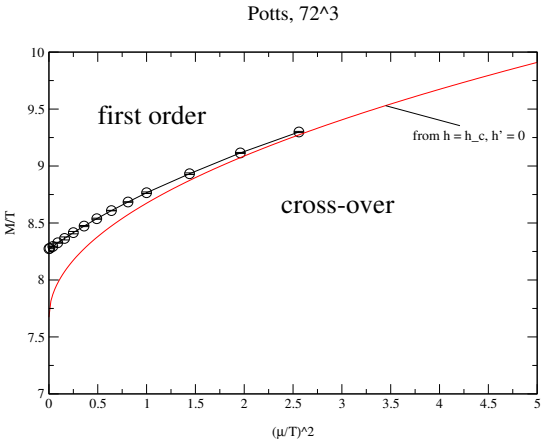

Figure 3: M/T for 2nd order transition vs. $(\mu/T)^2$

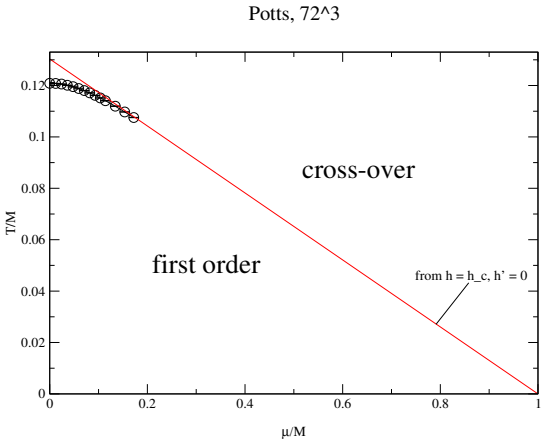

Figure 4: T/M for 2nd order transition vs. μ/M

Figure (3) suggests an interesting comparison with the finite temperature QCD phase diagram. Let us imagine increasing the chemical potential from zero, following the arrow in Figure (5). Without chemical potential, the quark mass is chosen such that the transition is first order. With a non-zero chemical potential, this first order phase transition weakens. At a certain chemical potential, the system shows a second order phase transition. With chemical potential larger than

this critical value, the system shows a cross-over. On the other hand, consider Figure (6) which is analogous to Figure (5). This figure is a schematic phase diagram for three-flavor QCD with *light* quarks suggested in [9] and summarizes the conventional wisdom. Without chemical potential, 3-flavor QCD shows a first order phase transition when the quark mass is smaller than a certain mass ($m_c(0)$). Let us say that we start with a system where the quark mass is larger than $m_c(0)$. Then, this 3-flavor QCD system has a cross-over. In this case, increasing the chemical potential makes the transition stronger: a second order phase transition appears when the chemical potential hits a certain magnitude. If the chemical potential is increased further, the system undergoes a first order phase transition. Therefore, the 3 light flavor QCD system shows (cross-over $\rightarrow$ second order phase transition $\rightarrow$ first order phase transition) as the chemical potential is increased. In contrast, the heavy quark QCD system suggested by 3-D $Z(3)$ Potts model will undergo (first order phase transition $\rightarrow$ second order phase transition $\rightarrow$ cross-over) as the chemical potential is increased. Interestingly, some recent light-quark QCD simulations give support to the possibility that the conventional wisdom scenario above might be at fault [10], so that the influence of the chemical potential in the light-quark and the heavy-quark cases would be similar.

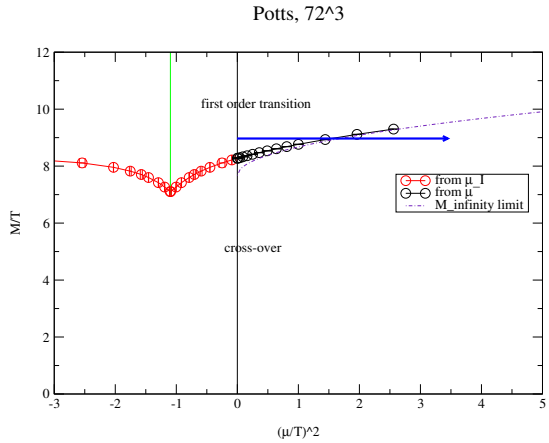

Figure 5: M/T for critical point vs. $(\frac{\mu}{T})^2$

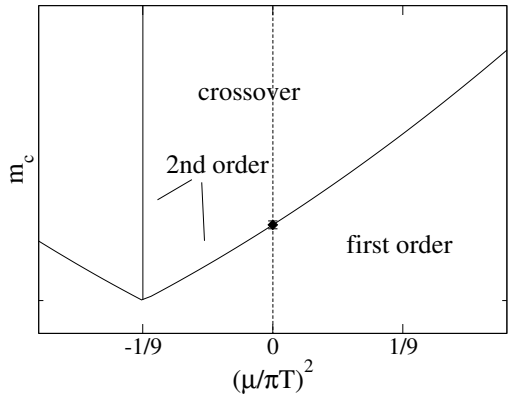

Figure 6: schematic QCD phase diagram for 3 light quarks

3. Imaginary vs Real Chemical Potential

For the case of an imaginary chemical potential, one can perform a direct sampling of Eq. (1.2), or reweight the $h = h'$ data used for the real chemical potential study. As before, the critical point is located by use of the magnetization Binder cumulant and $B_4 = 1.604$ crossing point.

In Figure (5), we put together the critical end point parameters obtained from the imaginary chemical potential case and those from the real chemical potential case (note the similarity with the schematic phase diagram for 3 light flavor QCD shown in Figure (6)). Although the proximity of the Roberge-Weiss transition at $\mu_I = \pi/3$ introduces curvature in the imaginary chemical potential result, the small real μ result is smoothly connected to the small imaginary μ_I result and the analytic continuation poses no serious problem even on a large lattice volume such as 72^3. However, the critical line shows significant curvature, which limits the accuracy of the extrapolation from imaginary

to real μ. A 4th order polynomial $\frac{M}{T} = 8.273 + 0.585(\frac{\mu}{T})^2 - 0.174(\frac{\mu}{T})^4 + 0.160(\frac{\mu}{T})^6 - 0.071(\frac{\mu}{T})^8$ is necessary to describe the critical line from $(\frac{\mu}{T})^2 = -(\frac{\pi}{3})^2$ to 1.5.

4. Summary

We extend earlier work on the 3-D $Z(3)$ Potts model with one external field coupled to $\Phi(\vec{x}) + \Phi^*(\vec{x})$ [4] or to $\Phi(\vec{x})$ [3] to the full general case $h\Phi(\vec{x}) + h'\Phi^*(\vec{x})$, and present a complete picture of the phase diagram in the (κ, h, h') parameter space. Our investigation also gives us a handle on heavy quark QCD at finite density and temperature which shares the same global symmetry, allowing us to make statements about the heavy quark QCD phase diagram in the finite temperature, finite density, and heavy quark mass parameter space.

For a real chemical potential, the partition function of the Potts model is shown to be real even though the action itself is complex. The sign problem is mild, and simulation results show that turning on a chemical potential μ makes the finite temperature transition weaker, so that the region of parameter space corresponding to a first-order transition shrinks under the influence of μ. This implies that a similar phenomenon occurs in the phase diagram of heavy quark QCD.

For an imaginary chemical potential, the action of the Potts model is real and the model is easy to study. Since both real chemical potential and imaginary chemical potential can be simulated, analytic continuation from imaginary to real chemical potential can be tested. We find that analytic continuation works satisfactorily, even with large lattice volumes such as 72^3.

In short, the 3-D $Z(3)$ Potts model has a rich structure and provides us with a useful "proving ground" for studying the finite temperature/density phase structure of QCD.

References

[1] P. Hasenfratz et al, *The SU(3) deconfinement phase transition in the presence of quarks*, *Phys. Lett.* **B133** (1983) 221.

[2] C. Alexandrou et al, *The deconfinement phase transition in one flavor QCD*, *Phys. Rev.* **D60** (1999) 034504.

[3] M. Alford et al, *Solution of the complex action problem in the Potts model for dense QCD*, *Nucl. Phys.* **B602** (2001) 61.

[4] F. Karsch and S. Stickan, *The three-dimensional three state Potts model in an external field*, *Phys. Lett.* **B488** (2000) 319.

[5] A. Roberge and N. Weiss, *Gauge theories with imaginary chemical potential and the phases of QCD*, *Nucl. Phys.* **B275** (1986) 734.

[6] P. Giudice and A. Papa, *Real and imaginary chemical potential in two color QCD*, *Phys. Rev.* **D69** (2004) 094509

[7] V. Azcoiti et. al, *Finite density QCD: a new approach*, *JHEP* **0412** (2004) 010

[8] R. H. Swendsen and J.Wang, *Nonuniversal critical dynamics in Monte Carlo simulations*, *Phys. Rev. Lett.* **58** (1987) 86.

[9] Ph. de Forcrand and O. Philipsen, *The QCD phase diagram for three degenerate flavors and small baryon density*, *Nucl. Phys.* **B673** (2003) 170

[10] O. Philipsen, these proceedings.